https://doi.org/10.17221/257/2020-CJFS

Mathematical models to describe the drying process of *Moringa oleifera* leaves in a convective-air dryer

*Kivaandra Dayaa Rao Ramarao, Zuliana Razali, Chandran Somasundram**

Institute of Biological Sciences, Faculty of Science, University of Malaya, Kuala Lumpur, Malaysia

**Corresponding author: chandran@um.edu.my*

Citation: Ramarao K.D.R., Razali Z., Somasundram C. (2021): Mathematical models to describe the drying process of *Moringa oleifera* leaves in a convective-air dryer. Czech J. Food Sci., 79: 000–000.

Abstract: Drying kinetics of Malaysian *Moringa oleifera* leaves was investigated using a convective-air dryer. The drying parameters were: temperature (40, 50, 60, 70 °C), air velocity (1.3 m s^{-1}, 1.7 m s^{-1}). The drying process took place in the falling rate period and there was an absence of a constant rate period in this experiment. Six mathematical models (Lewis, Henderson and Pabis, Wang and Singh, Peleg, Page, and logarithmic) were selected for the description of drying characteristics of the leaves. The Wang and Singh model was determined as the best model based on the highest overall coefficient determinant (R^2) and the lowest overall root mean square error (RMSE). The effective diffusivity (D_{eff}) was also calculated which was in the range of 3.98 × 10^{-11} m^2 s^{-1} to 1.74 × 10^{-10} m^2 $s^{-1.}$ An Arrhenius relation was constructed to determine the activation energy for the samples in the convective air dryer. The activation energy for *M. oleifera* leaves was 39.82 kJ mol^{-1} and 33.13 kJ mol^{-1} at drying velocities of 1.3 m s^{-1} and 1.7 m s^{-1}, respectively.

Keywords: drying kinetics; convective-air drying; mathematical modelling; effective diffusivity; activation energy

Moringa oleifera is a widely cultivated species of the genus *Moringa* in the family Moringaceae. Various parts of the tree can be used in food, medicine, and many more applications (Premi et al. 2010). *M. oleifera* leaves are considered full of medicinal properties due to their rich source of vitamins, micronutrients, protein, and minerals (Ma et al. 2020). The leaves are usually prepared by drying followed by crushing into a powdered form which can then be stored for months without compromising nutritional values (Suzaudduła et al. 2019). The multitude of medicinal properties in the leaves is believed to have been contributed by its wide range of phytochemicals such as flavonoids, phenols, and alkaloids (Fahal et al. 2018).

Drying is a common technique utilised in the postharvest preservation of food products (Chua et al. 2019). Moisture is removed during the drying process by simultaneous heat and mass transfer from a drying product. During the process of drying, water leaves the food product which reduces the chances of microorganism growth and unfavourable chemical reactions, thereby extending the shelf-life and at times contributing to increased nutritional properties of the dried product (Minaei et al. 2012). The recent COVID-19 pandemic caused many countries to enforce lockdown policies and this has caused various unsold postharvest products like vegetables and fruits to be discarded. Therefore, it is crucial for food industries to maintain food products and drying enables long-term storage of those products. Different drying methods have been developed amongst which the convective hot air-drying system is one of the most employed methods (Chua et al. 2019). Mathematical models are required to predict the drying behaviour of a food product so that optimum drying operating conditions can be determined as drying kinetics is a complicated phenomenon (Minaei et al. 2012). There are various studies regarding the drying behaviour of leaves, for instance, *M. oleifera* leaves (Premi et al. 2010), peppermint leaves (Ashtiani et al. 2017), and Moldavian dragonhead leaves (Rudy et al. 2020). The objective of this study was to: *i*) dry local (Malaysian) *M. oleifera* leaves in a self-built prototype convective air-dryer and determine the effects of drying

https://doi.org/10.17221/257/2020-CJFS

temperature and air velocity on its drying characteristics, *ii*) to employ six different mathematical models available from literature to describe the drying characteristics, *iii*) to calculate effective diffusivity and activation energy of the leaves.

MATERIAL AND METHODS

Convective-air dryer. A prototype benchtop convective dryer designed and built in the Postharvest Biotechnology Laboratory, University of Malaya, Malaysia was used for the drying experiments. The schematic layout of the benchtop dryer is shown in Figure 1, where it consists of (a) a hot air supply controlled by a motor, (b) cover, (c) three-legged stand, (d) drying tray, (e) water retention tray, (f) air inlet and (g) central supporting rod made of stainless steel. The outer cover and inner material are made of polyethylene terephthalate (PET) and thermostable aluminium foil, respectively. The outer cover has 9 outlets (15 mm each) made of aluminium alloy to allow hot air to be removed from the dryer during its operation. The drying tray and retention tray are made from high-density polyethylene and polypropylene, respectively. The drying tray has 2 378 pores (3 × 7 mm each) to ensure hot air can reach the drying product efficiently. The dryer's motor (Figure 1a) is capable of producing two different air velocities at 1.3 m s^{-1} (for velocity 1) and 1.7 m s^{-1} (for velocity 2). The temperature used in this experiment ranges from 40 °C to 80 °C.

Sample preparation. *M. oleifera* leaves were used as the sample for this study. Fresh leaves were purchased from a local market in Petaling Jaya, Malaysia located approximately 6 km away from the Postharvest Laboratory, University of Malaya, Malaysia. The leaves were removed from the stem by hand. The leaf thickness was measured using a set of Vernier callipers (MDVC-150; MISUMI, Japan) with an average thickness of 0.1 mm for each leaf. The leaves were then evenly spread out onto two drying trays that were built into the convective dryer. The initial moisture contents (MC) of *M. oleifera* leaves were determined based on the Association of Official Analytical Chemists method (AOAC 2000).

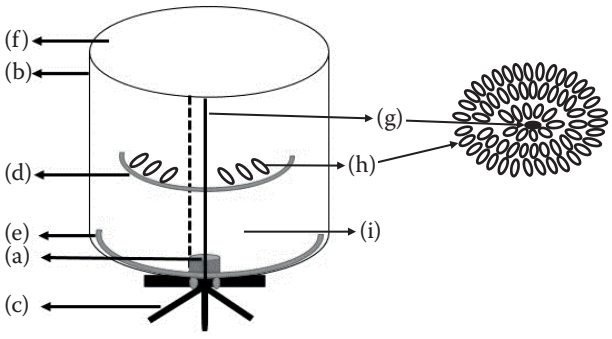

Figure 1. The schematic layout of the prototype convective air-dryer: (a) motor, (b) cover, (c) three-legged stand, (d) drying tray, (e) water retention tray, (f) air inlet, (g) central supporting rod made of stainless steel, (h) leaf orientation (leaves are arranged horizontally on the drying tray; note that the leaves are not drawn to scale), and (i) direction of hot air flow from the motor

Drying experiment. Four different temperatures (40, 50, 60, 70 °C) were used for this experiment and this range was selected according to Ali et al. (2014), Taheri-Garavand and Meda (2018), and Turan and Firatligil (2019). Temperatures above 70 °C were avoided as they can lead to a nutritional loss in the leaves (Olabode et al. 2015). Before the drying process began, the dryer was turned on for at least one hour to obtain a steady state. The leaves were laid in the drying tray parallel to the wind stream from the motor. The leaves were removed from the drying tray every 10 min and weighed using an analytical balance (ME104T; Mettler Toledo, Malaysia). Drying was continued until a constant weight was achieved. The initial weight and final weight (after drying) of the leaves were recorded.

Mathematical modelling of drying curves. The moisture ratio (MR) and drying rate (DR) curves were constructed using the following equations:

$$MR = \frac{M_t - M_{eq}}{M_0 - M_{eq}} \quad (1)$$

where: MR – moisture ratio; M_t, M_0, M_{eq} – MC at any given time, initial MC, and equilibrium MC, respectively [% wet basis (w.b.)] (Ashtiani et al. 2017).

For longer drying times, since M_{eq} is smaller than both M_t and M_0, so Equation 1 can be simplified (Akpinar 2006; Ashtiani et al. 2017):

$$MR = \frac{M_t}{M_0} \quad (2)$$

Drying rate (DR) was expressed as [g^{-1} (water) g^{-1} (dry solids)] min^{-1}:

$$DR = \frac{M_1 - M_2}{t_2 - t_1} \quad (3)$$

where: DR – drying rate; t_1, t_2 – drying times (min); M_1, M_2 – MC [% dry basis (d.b.)] of *M. oleifera* leaves at time t_1 and t_2, respectively.

https://doi.org/10.17221/257/2020-CJFS

The drying data obtained was then fitted with several commonly used mathematical models involving agricultural products (Kashaninejad et al. 2007; Diamante et al. 2010; Kaleta and Górnicki 2010; Mercali et al. 2010; Perea-Flores et al. 2012; da Silva et al. 2013). The chosen models are shown below:

Model A) Lewis: $MR = \exp(-at)$
Model B) Henderson and Pabis: $MR = a\exp^{-bt}$
Model C) Wang and Singh: $MR = 1 + at + bt^2$
Model D) Peleg: $MR = 1 - t\,(a + bt)^{-1}$
Model E) Page: $MR = \exp^{-atb}$
Model F) Logarithmic: $MR = a\exp^{-bt} + c$

where: a, b and c – model constants; t – time (min).

The highest coefficient (R^2) and the lowest root mean square error (RMSE) were the criteria that must be met for the best model. RMSE was calculated as shown:

$$RMSE = \left[\frac{1}{N}\sum_{i=1}^{N}\left(MR_{pre,i} - MR_{\exp,i}\right)^2\right]^{1/2} \quad (4)$$

where: $RMSE$ – root mean square error; N – number of observations; MR_{pre} – predicted MR; MR_{exp} – experimental value of the MR.

Microsoft Excel Solver (Microsoft Excel 2016) was used for the nonlinear-regression analysis.

Effective diffusivity and activation energy. Fick's second law can be used to describe the drying behaviour of leaves as described in the literature (Lamharrar et al. 2017; Taheri-Garavand and Meda 2018). The equation is shown in Equation 5:

$$\ln(MR) = \ln(\frac{8}{\pi^2}) - \frac{\pi^2 D_{eff}\, t}{4L^2} \quad (5)$$

where: L – half the thickness (m) of *M. oleifera* leaves; D_{eff} – effective diffusion coefficient of dried *M. oleifera* leaves.

The plot of ln(MR) against time was used for calculation of D_{eff}, where the slope (D) based on Equation 5 would result in the following equation:

$$\ln(MR) = \ln(\frac{8}{\pi^2}) - \left(\frac{\pi^2 D_{eff}\, t}{4L^2}\right) \quad (6)$$

An Arrhenius type equation was used to model the effects of temperature on D_{eff}.

$$D_{eff} = D_0 \exp\left(-\frac{E_a}{R(T + 273.15)}\right) \quad (7)$$

where: D_0 – Arrhenius factor (m^2 s^{-1}); E_a – activation energy for the moisture diffusion (kJ mol^{-1}); R – gas constant [kJ (mol K)$^{-1}$]; T – temperature (°C).

Based on Equation 6, a straight line of ln(D_{eff}) against the inverse of absolute temperature was constructed where the value of E_a was obtained from the slope. Equation 7 is presented below:

$$\ln(D_{eff}) = \ln(D_0)\exp\left(-\frac{E_a}{R(T + 273.15)}\right) \quad (8)$$

RESULTS AND DISCUSSION

Drying of leaves. The drying curves of *M. oleifera* leaves dried at 40, 50, 60, 70 °C (air velocity: 1.3 m s^{-1} and 1.7 m s^{-1}) are presented in Figure 2. The curves were normalised as dimensionless MR data and analysed with drying time (Ashtiani et al. 2017). The MR curves for *M. oleifera* leaves dried at various temperatures and air velocities decreased with time (Figure 2). Based on Figure 2, the total time taken by the leaves dried at 40, 50, 60, and 70 °C and drying air velocity of 1.3 m s^{-1} to reach MC of 7.99, 8.36, 5.18, and 4.24% (w.b.) was 160, 130, 90, and 70 min, respectively, whereas the time taken to reach MC of 9.80, 9.27, 4.71, and 3.92% (w.b.) at drying air velocity of 1.7 m s^{-1} for the same temperatures were 110, 110, 70, and 60 min, respectively. To allow for a more precise comparison between drying time and the drying conditions, we looked at the drying time required to reach a fixed MC of approximately 10 (±1)% (w.b.). Results showed that the drying time for samples at 40, 50, 60, and 70 °C and drying air velocity of 1.3 m s^{-1} was 140, 110, 70, and 50 min, whereas drying time for samples at the same temperature range but drying air velocity of 1.7 m s^{-1} was 100, 100, 60, and 40 min. From Figure 2, higher drying air velocity also contributed to shorter drying time for the leaf samples, for instance, the drying time at 40 °C was recorded at 160 min (1.3 m s^{-1}) and 110 min (1.7 m s^{-1}), while at 70 °C the drying time was 70 min (1.3 m s^{-1}) and 60 min (1.7 m s^{-1}). These results were consistent with the drying experiments of Kashaninejad et al. (2007) on pistachio nuts, Premi et al. (2012) on *M. oleifera* leaves and Taheri-Garavand and Meda (2018) on savoury leaves in which they reported higher drying temperatures and velocities reduced drying times of the product. The reduced total drying time corresponding

https://doi.org/10.17221/257/2020-CJFS

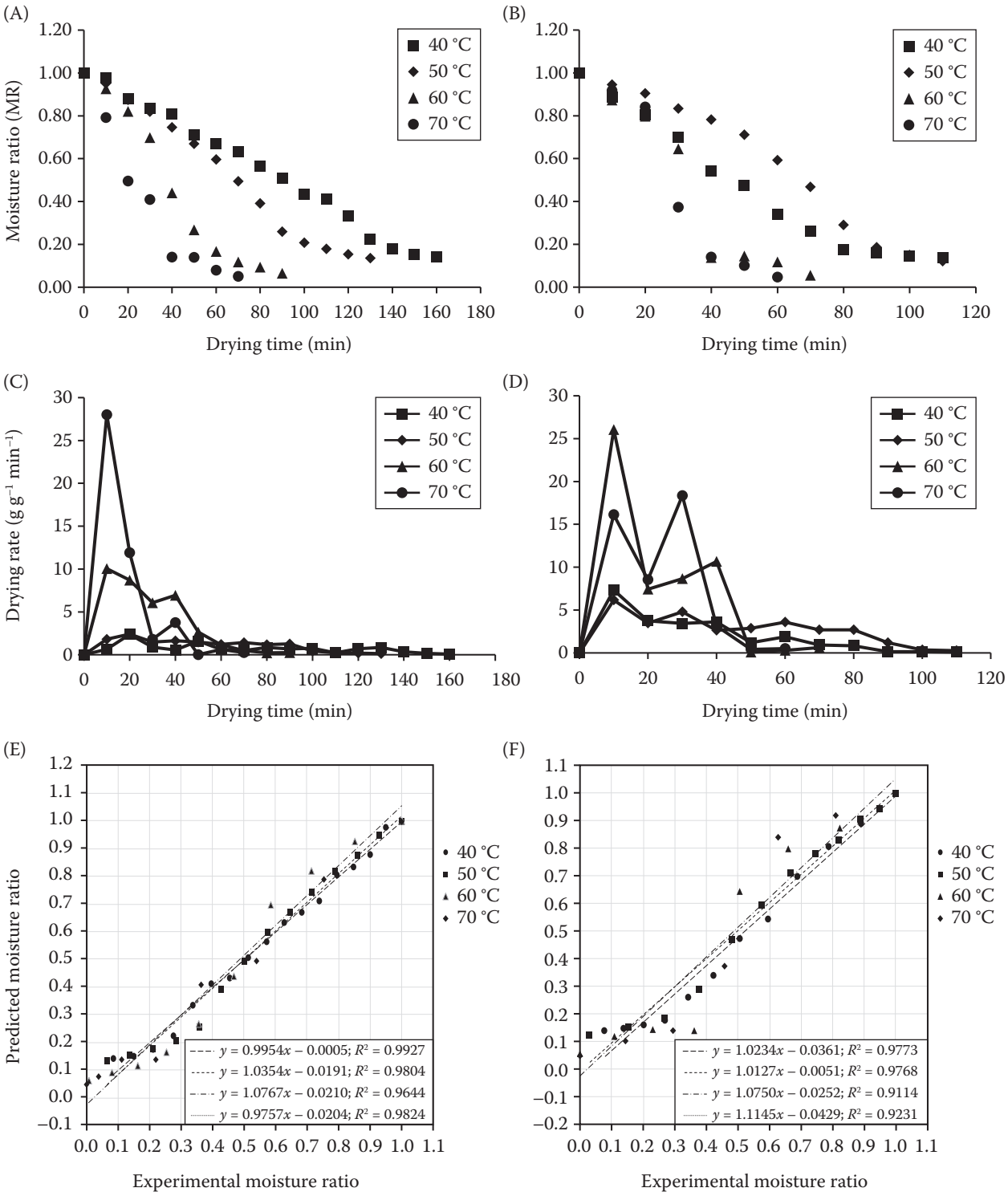

Figure 2. (A) MR of *Moringa oleifera* leaves dried at 1.3 m s^{-1}, (B) MR of *M. oleifera* leaves dried at 1.7 m s^{-1}, (C) DR curve of *M. oleifera* leaves dried at 1.3 m s^{-1}, (D) DR curve of *M. oleifera* leaves dried at 1.7 m s^{-1}, (E) experimental MR *versus* predicted (Wang and Singh model) MR values for different air temperatures (drying air velocity: 1.3 m s^{-1}), (F) **e**xperimental MR *versus* predicted (Wang and Singh model) MR values for different air temperatures (drying air velocity: 1.7 m s^{-1})

MR – moisture ratio; DR – drying rate

https://doi.org/10.17221/257/2020-CJFS

to higher temperatures could be caused by increased heat transfer inside the product which causes moisture to migrate more rapidly to the leaf surface, followed by a higher reduction in external resistance for mass transfer at higher drying air velocities that increases DR (Premi et al. 2012; Taheri-Garavand and Meda 2018). From the DR curve in Figure 2, a constant rate period was absent and drying took place predominantly in the falling rate period at different temperatures and air velocities. An initial increase in the DR occurred during the early stages of drying for all drying temperatures. The DR curves obtained in Figure 2 agrees with previous research conducted on basil, parsley, and mint leaves (Akpinar 2006), *M. oleifera* leaves (Ali et al. 2014) and savoury leaves (Taheri-Garavand and Meda 2018). Drying mainly took place in the falling rate period except for the initial stages where an acceleration period was observed. During the falling rate period, the movement of moisture from the leaf's interior to its surface is governed by diffusion since the leaf surface is not water-saturated anymore (Doymaz 2005; Akpinar 2006). The DR decreased towards the end of drying, and this is mainly caused by the decreasing MR (Figure 2) and reduced migration rate of moisture from the leaf's interior to the surface (Premi et al. 2012).

Mathematical modelling. Table 1 shows the statistical results (R^2, *RMSE*) for modelling. The model with the highest overall value of R^2 and lowest overall value of *RMSE* for drying temperature and air velocity is the Wang and Singh model (R^2 = 0.9880; *RMSE* = 0.02102). From Table 1, the values of R^2 and *RMSE* obtained from this model for drying air velocity of 1.3 m s^{-1} and 1.7 m s^{-1} for temperatures of 40, 50, 60, and 70 °C range from R^2 = 0.9434 to 1.0000, and *RMSE* = 0.0057 – 0.0429. When considering each drying condition, the average R^2 for the Wang and Singh Model is 0.9880, and the average *RMSE* = 0.0210. These values fit the criteria set for the best model, which is the highest R^2 and lowest *RMSE* values. Therefore, this model is the most suitable to represent the drying behaviour of *M. oleifera* leaves in our convective-air type dryer. Figures 2E and 2F show the experimental MR *versus* predicted (Wang and Singh model) MR values for different air temperatures and drying velocities of 1.3 m s^{-1} and 1.7 m s^{-1}, respectively. The R^2 values obtained were all above 0.9, indicating a good fit of the data.

Effective moisture diffusivity and activation energy. The results of this experiment showed the presence of a falling rate drying period which affected the drying time, indicating internal mass transfer resistance which enables the interpretation of experimental re-

Table 1. The fitness of various mathematical models for *Moringa oleifera* leaves at different temperatures and air velocities

v (m s^{-1})	*T* (°C)	Model	Model constant	R^2	*RMSE*
1.3	40	A	a = 0.0086	0.9664	0.0181
		B	a = 1.0000 b = 0.0086	0.9664	0.0181
		C	a = –0.0053 b = –2.75 × 10^{-6}	0.9996	0.0057
		D	a = 149.6057 b = 0.1303	0.9987	0.0127
		E	a = 0.0015 b = 1.2800	0.9974	0.0207
		F	a = 10.3202 b = 0.0006 c = –9.3202	0.9999	0.0061
1.7	40	A	a = 0.0170	0.9390	0.0162
		B	a = 1.0000 b = 0.0170	0.9390	0.0162
		C	a = –0.0111 b = 2.5 × 10^{-5}	0.9919	0.0150
		D	a = 98.3430 b = 0.1458	0.9803	0.0120
		E	a = 0.0118 b = 1.0850	0.9510	0.0131
		F	a = 1.3879 b = 0.0099 c = –0.3879	0.9778	0.0114
1.3	50	A	a = 0.0116	0.9596	0.0233
		B	a = 1.0000 b = 0.0116	0.9596	0.0234
		C	a = 0.0071 b = 1.02 × 10^{-6}	1.0000	0.0117
		D	a = 135.7110 b = 0.0239	1.0000	0.0115
		E	a = 0.0113 b = 1.0001	0.9617	0.0230
		F	a = 6.6208 b = 0.0011 c = –5.6208	0.9996	0.0116
1.7	50	A	a = 0.0118	0.9690	0.0351
		B	a = 1.0000 b = 0.0118	0.9690	0.0351
		C	a = –0.0064 b = 3.84 × 10^{-5}	0.9864	0.0139
		D	a = 92.0103 b = 0.1764	0.9891	0.0149

https://doi.org/10.17221/257/2020-CJFS

Table 1. To be continued

v (m s^{-1})	T (°C)	Model	Model constant	R^2	*RMSE*
1.7	50	E	a = 0.0088 b = 1.0849	0.9738	0.0327
		F	a = 3.5828 b = 0.0024 c = −2.5828	0.9986	0.0228
1.3	60	A	a = 0.0218	0.9319	0.0340
		B	a = 1.0000 b = 0.0218	0.9319	0.0340
		C	a = −0.0152 b = 4.6 × 10^{-5}	0.989	0.0227
		D	a = 66.4313 b = 0.2463	0.9935	0.0235
		E	a = 0.0147 b = 1.0811	0.9513	0.0316
		F	a = 2.1767 b = 0.0069 c = −1.9521	0.9924	0.0233
1.7	60	A	a = 0.0271	0.9340	0.0512
		B	a = 1.0000 b = 0.0271	0.9340	0.0512
		C	a = −0.0180 b = 5.4 × 10^{-5}	0.9944	0.0400
		D	a = 56.4473 b = 0.1721	0.9970	0.0402
		E	a = 0.0002 b = 2.3995	0.9599	0.0283
		F	a = 2.9521 b = 0.0060 c = −1.9521	0.9964	0.0402
1.3	70	A	a = 0.0361	0.8915	0.0201
		B	a = 1.0000 b = 0.0361	0.8915	0.0200
		C	a = −0.0265 b = 0.0002	0.9434	0.0163
		D	a = 49.9866 b = 0.2237	0.9403	0.0181
		E	a = 0.0234 b = 1.0039	0.9487	0.0491
		F	a = 1.1483 b = 0.0273 c = −0.1483	0.9331	0.0166
1.7	70	A	a = 0.0304	0.9376	0.0593
		B	a = 1.0000 b = 0.0271	0.9493	0.0610

Table 1. To be continued

v (m s^{-1})	T (°C)	Model	Model constant	R^2	*RMSE*
1.7	70	C	a = −0.0194 b = 4.6 × 10^{-5}	0.9995	0.0429
		D	a = 54.5464 b = 0.0539	0.9997	0.0430
		E	a = 6.04 × 10^{-5} b = 2.8023	0.9509	0.0196
		F	a = 6.9652 b = 0.0027 c = −5.9652	0.9995	0.0430

v – drying air velocity; T – temperature; *RMSE* – root mean square error

sults using Fick's law as described in Equation 5 (Premi et al. 2010). Table 2 shows the D_{eff} values for *M. oleifera* leaves dried in a convective-air dryer. Based on Table 2, the D_{eff} values for samples dried at different temperatures with constant air velocity of 1.3 m s^{-1} ranged from 3.98 × 10^{-11} m^2 s^{-1} to 1.41 × 10^{-10} m^2 s^{-1}, while samples dried at different temperatures at a constant air velocity of 1.7 m s^{-1} ranged from 6.43 × 10^{-11} m^2 s^{-1} to 1.74 × 10^{-10} m^2 s^{-1}. This range falls within 10^{-11} m^2 s^{-1} to 10^{-9} m^2 s^{-1} for food materials (Zogzas et al. 1996). The results showed that air velocity can affect the D_{eff} values, and this phenomenon was explained by Mirzaee et al. (2009), whereby drying air velocity affects how much of that drying air comes into contact with the sample's surface, which results in changes to the sample's moisture gradient and thus affecting the moisture diffusivity. From Table 2, the D_{eff} values increased as the drying temperature increased except for samples dried at 1.7 m^2 s^{-1} with dying temperatures of 40 °C and 50 °C, where the D_{eff} value decreased slightly from

Table 2. Effective diffusivities of *Moringa oleifera* leaves in different drying conditions

T (°C)	v (m s^{-1})	D_{eff}
40	1.3	3.98 × 10^{-11}
	1.7	6.53 × 10^{-11}
50	1.3	5.38 × 10^{-11}
	1.7	6.43 × 10^{-11}
60	1.3	1.06 × 10^{-10}
	1.7	1.40 × 10^{-10}
70	1.3	1.41 × 10^{-10}
	1.7	1.74 × 10^{-10}

T – temperature; v – drying air velocity; D_{eff} – effective diffusivity

https://doi.org/10.17221/257/2020-CJFS

6.53×10^{-11} m^2 s^{-1} to 6.43×10^{-11} m^2 s^{-1}, respectively. This may be due to higher temperatures having higher heat energy, which increases water molecule activity in the leaf sample, and from higher vapour pressure that accelerated moisture transfer (Ashtiani et al. 2017). Based on the Arrhenius plot (Figure 3), the activation energy values were 39.82 kJ mol^{-1} and 33.13 kJ mol^{-1} for drying velocities of 1.3 m s^{-1} and 1.7 m s^{-1}, respectively These values are within 12.7–110 kJ mol^{-1}, which is considered the general range for food materials (Zogzas et al. 1996; Xiao et al. 2012). The activation energy of *M. oleifera* leaves decreased as the drying air velocity was increased. This trend was like those of Ashtiani et al. (2017) for peppermint leaves. The values were in reasonable agreement with other studies like 32.74 kJ mol^{-1} for *M. oleifera* leaves (Premi et al. 2012), 33.4 kJ mol^{-1} for *Andrographis paniculata* (Hee and Chong 2015) and 37.98 kJ mol^{-1} for quinoa (Gely and Santalla 2007).

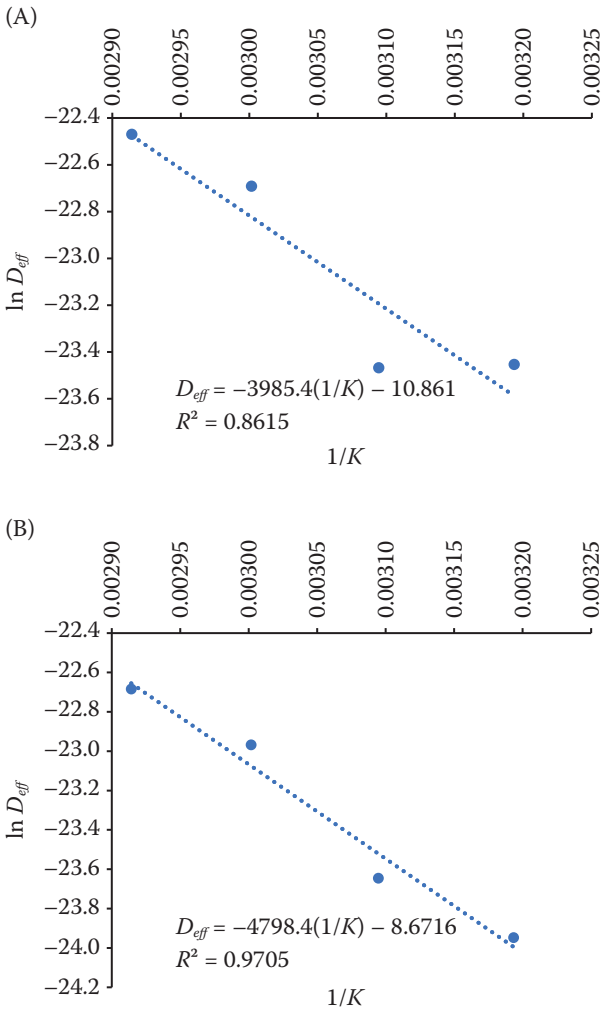

Figure 3. Arrhenius-type relationship between effective diffusivity and temperature: (A) air velocity = 1.3 m s^{-1}, (B) air velocity = 1.7 m s^{-1}

D_{eff} – effective diffusivity; K – temperature (Kelvin)

CONCLUSION

A prototype convective drying system was developed for the drying of *M. oleifera* leaves. The drying kinetics of the leaves were investigated. The convective air drying of *M. oleifera* leaves took place during the falling rate period, indicating internal diffusion as the mechanism which controlled moisture removal from the leaves. Drying time decreased as the drying air temperature and velocity was increased. Statistical analysis showed that the Wang and Singh model showed the best fit among the selected models for describing the drying behaviour of *M. oleifera* leaves. The effective moisture diffusivity ranged from 6.43×10^{-11} m^2 s^{-1} to 1.74×10^{-10} m^2 s^{-1}. Effective moisture diffusivity of *M. oleifera* leaves increased as drying temperature increased, and an Arrhenius-type equation adequately described temperature dependence of D_{eff} where the activation energy was 39.82 kJ mol^{-1} and 33.13 kJ mol^{-1} for *M. oleifera* leaves dried at velocities of 1.3 m s^{-1} and 1.7 m s^{-1}, respectively. This study provided useful information to the literature on drying of *M. oleifera* leaves using the convective-air drying method. The prototype convective-air dryer can be further modified according to information from this research if the need arises for commercial purposes.

REFERENCES

Akpinar E.K. (2006): Mathematical modelling of thin layer drying process under open sun of some aromatic plants. Journal of Food Engineering, 77: 864–870.

Ali M., Yusof Y., Chin N., Ibrahim M., Basra S. (2014): Drying kinetics and colour analysis of *Moringa oleifera* leaves. Agriculture and Agricultural Science Procedia, 2: 394–400.

Ashtiani S.H.M., Salarikia A., Golzarian M.R. (2017): Analyzing drying characteristics and modeling of thin layers of peppermint leaves under hot-air and infrared treatments. Information Processing in Agriculture, 4: 128–139.

Chua L.Y., Chong C.H., Chua B.L., Figiel A. (2019): Influence of drying methods on the antibacterial, antioxidant and essential oil volatile composition of herbs: A review. Food and Bioprocess Technology, 12: 450–476.

da Silva W.P., de Silva C.M., de Sousa J.A., Farias V.S. (2013): Empirical and diffusion models to describe water transport into chickpea (*Cicer arietinum* L.). International Journal of Food Science and Technology, 48: 267–273.

https://doi.org/10.17221/257/2020-CJFS

Diamante L.M., Ihns R., Savage G.P., Vanhanen L. (2010): A new mathematical model for thin layer drying of fruits. International Journal of Food Science and Technology, 45: 1956–1962.

Doymaz I. (2005): Sun drying of figs: An experimental study. Journal of Food Engineering, 71: 403–407.

Fahal M., Rani B., Aklakur M., Chanu T., Saharan N. (2018): Qualitative and quantitative phytochemical analysis of *Moringa oleifera* (Lam) Pods. International Journal of Current Microbiology and Applied Sciences, 7: 657–665.

Gely M.C., Santalla E.M. (2007): Moisture diffusivity in quinoa (*Chenopodium quinoa* Willd.) seeds: Effect of air temperature and initial moisture content of seeds. Journal of Food Engineering, 78: 1029–1033.

Hee Y.Y., Chong G.H. (2015): Drying behaviour of *Andrographis paniculata* in vacuum drying. International Food Research Journal, 22: 393–397.

Kaleta A., Górnicki K. (2010): Evaluation of drying models of apple (var. McIntosh) dried in a convective dryer. International Journal of Food Science and Technology, 45: 891–898.

Kashaninejad M., Mortazavi A., Safekordi A., Tabil L.G. (2007): Thin-layer drying characteristics and modeling of pistachio nuts. Journal of Food Engineering, 78: 98–108.

Lamharrar A., Idlimam A., Alouani A., Kouhila M. (2017): Modelling of thin layer solar drying kinetics and effective diffusivity of *Urtica dioica* leaves. Jounal of Engineering Science and Technology, 12: 2141–2153.

Ma Z.F., Ahmad J., Zhang H., Khan I., Muhammad S. (2020): Evaluation of phytochemical and medicinal properties of Moringa (*Moringa oleifera*) as a potential functional food. South African Journal of Botany, 129: 40–46.

Mercali G.D., Tessaro I.C., Noreña C.P., Marczak L.D. (2010): Mass transfer kinetics during osmotic dehydration of bananas (*Musa sapientum*, shum.). International Journal of Food Science and Technology, 45: 2281–2289.

Minaei S., Motevali A., Najafi G., Mousavi Seyedi S.R. (2012): Influence of drying methods on activation energy, effective moisture diffusion and drying rate of pomegranate arils (*'Punica granatum'*). Australian Journal of Crop Science, 6: 584–591.

Mirzaee E., Rafiee S., Keyhani A., Emam-Djomeh Z. (2009). Determining of moisture diffusivity and activation energy in drying of apricots. Research in Agricultural Engineering, 55: 114–120.

Olabode Z., Akanbi C., Olunlade B., Adeola, A. (2015). Effects of drying temperature on the nutrients of Moringa (*Moringa oleifera*) leaves and sensory attributes of dried leaves infusion. Direct Research Journal of Agriculture and Food Science, 3: 177–122.

Perea-Flores M.J., Garibay-Febles V., Chanona-Perez J.J., Calderon-Dominguez G., Mendez-Mendez J.V., Palacios--González E., Gutierrez-Lopez G.F. (2012): Mathematical modelling of castor oil seeds (*Ricinus communis*) drying kinetics in fluidized bed at high temperatures. Industrial Crops and Products, 38: 64–71.

Premi M., Sharma H., Sarkar B., Singh C. (2010): Kinetics of drumstick leaves (*Moringa oleifera*) during convective drying. African Journal of Plant Science, 4: 391–400.

Premi M., Sharma H., Upadhyay A. (2012): Effect of air velocity and temperature on the drying kinetics of drumstick leaves (*Moringa oleifera*). International Journal of Food Engineering, 8.

Rudy S., Dziki D., Biernacka B., Krzykowski A., Rudy M., Gawlik-Dziki U., Kachel M. (2020): Drying characteristics of *Dracocephalum moldavica* leaves: Drying kinetics and physicochemical properties. Processes, 8: 509.

Suzauddula M., Miah M.M., Mukta N.A., Kamrul N., Hossain M.B. (2019): Kinetics study on dried *Moringa oleifera* leaves during sun drying, multi commodity solar tunnel dryer drying and oven drying. Malaysian Journal of Halal Research, 2: 10–15.

Taheri-Garavand A., Meda V. (2018): Drying kinetics and modeling of savory leaves under different drying conditions. International Food Research Journal, 25: 1357–1364.

Turan O.Y., Firatligil F.E. (2019): Modelling and characteristics of thin layer convective air-drying of thyme (*Thymus vulgaris*) leaves. Czech Journal of Food Science, 37: 128–134.

Xiao H.W., Yao X.D., Lin H., Yang W.X., Meng J.S., Gao Z.J. (2012): Effect of SSB (superheated steam blanching) time and drying temperature on hot air impingement drying kinetics and quality attributes of yam slices. Journal of Food Process Engineering, 35: 370–390.

Zogzas N., Maroulis Z., Marinos-Kouris D. (1996): Moisture diffusivity data compilation in foodstuffs. Drying technology, 14: 2225–2253.

Received: October 23, 2020
Accepted: September 5, 2021